

A Simple but Effective Denoising Algorithm in Projection Domain of CBCT

Shaojie Chang, Yanbo Zhang, Ti Bai, Xi Chen,
Qiong Xu, and Xuanqin Mou^(✉)

Institute of Image Processing and Pattern Recognition,
Xi'an Jiaotong University, Xi'an 710049, Shaanxi, China
shaojie_chang@foxmail.com, yanbozhang007@163.com,
baiti018@stu.mail.xjtu.edu.cn, {xi.chen,xuqiong,xqmou}@mail.xjtu.edu.cn

Abstract. There are growing concerns on the potential side effect of radiation, which could be decreased by lowering the tube current. However, this manner will lead to a degraded image since X-ray imaging is a quantum accumulation process. Great efforts have been devoted to alleviate this problem. In this paper, a simple Wiener filter was employed to denoise projection data in detector domain. And then an enhancement filter was exploited to strengthen small structures. As a consequence, this combination led to a reconstruction with good trade-off between noise and resolution. For the purpose of comparison, block-matching and 3D/4D denoising algorithm (BM3D/BM4D) were also adopted to denoise the projections. Experimental results demonstrated that the proposed algorithm could deliver a reconstruction with comparable quality as BM4D algorithm while better than that of BM3D denoising algorithm. Note that the propose algorithm has a much higher computation efficiency than BM3D/BM4D, and hence provides an insight into the clinical utility where real time is of high importance.

Keywords: CBCT · Noise reduction · BM3D · BM4D · Wiener filter · Image enhancement

1 Introduction

Cone beam computed tomography (CBCT) has been widely used in clinics, such as for position in radiation therapy and for dental disease diagnosis, and etc. However, it is well-known that X-ray radiation is harmful to human body by inducing genetic, cancerous and other diseases. Hence, it is essential to reduce the radiation dose as low as reasonably achievable (ALARA). A natural idea is to lower the radiation exposure, however, since X-ray imaging is a quantum accumulation process, this manner will unavoidably decrease the signal-noise-ratio (SNR) of the measurements which would lead to a degraded image.

Great efforts have been devoted to alleviate this problem. It is common to divide them into three categories [1]: (a) raw data denoising then reconstruction, (b) reconstruction then denoising in image domain, (c) iterative reconstruction [6], among which, the first two have a high computation efficiency due

to that no forward/backward projection operators are involved. In this work, we will focus on developing a raw data denoising algorithm which can deliver a reconstruction with good tradeoff between noise and resolution.

By exploiting the correlation between neighbour detectors, an ensemble of raw data/projection denoising algorithms have been proposed. A filter proposed by Hsieh *et al.* [2], whose parameters are dynamically adapted to the local noise characteristics, was employed on sinogram denoising. Kachelriess *et al.* extended this filter into the three dimensional case [3]. Taking the stochastic properties of noise into consideration, Jing Wang *et al.* proposed the penalized weighted least-squares (PWLS) algorithm to denoise the raw data [1]. A. Manduca and J. Trzasko [5] utilized a weighted average filter in local neighborhood based on spatial proximity and intensity similarity to smooth the sinogram. Aim at relieving at this problem, in this paper, we propose a simple but effective projection denoising algorithm which can deliver a reconstruction with good trade-off between noise and resolution.

2 Methods and Materials

In this work, we denote by detector domain a certain two dimensional (2D) CBCT projection data, while angle domain represents data of a specific detector bin in different views.

2.1 Projection Correlation in Detector Domain

It is well-known that natural images are high dimensional signals which contain a rich amount of redundancies due to that strong correlations exist among neighbour pixels [9], base on which, a multitude of denoising algorithms have been proposed in the field of image processing, such as total variation minimization [8]. Moreover, patch level structure similarities also have been employed to facilitate the denoising algorithm, among them, block-matching and 3D filtering (BM3D) [10] is proved to be quite efficient for denoising a natural image with abundant structures. However, the drawback of BM3D is its low computational speed because block matching process is very time-consuming.

In the context of CBCT, in contrast to the object needed to be imaged, no distinct structures exist on the projection data in detector domain due to the intrinsic property of line integral, not to mention the effect of scatter which would induce additional smooth. This maybe potentially degrades the performance of those block based denoising algorithms, such as dictionary learning [7] based and BM3D, which have been validated their efficiencies in natural image processing.

2.2 Wiener Filter

Despite this fact, strong correlations still could be observed from data in detector domain, especially for CBCT projections. On the other hand, Wiener filter, which is very simple, stable and fast, has been proved to an optimal adaptive

filter in the field of signal processing. Motivated by these, in this work, Wiener filter is employed to remove noise contained in detector domain data. Basically, Wiener filter can be expressed as follows:

$$P_{wiener} = \mu_m + \frac{\max(0, \sigma_m^2 - v^2)}{\max(\sigma_m^2, v^2)} (P_{raw} - \mu_m) \quad (1)$$

where P_{raw} represents the raw data in detector domain. Denoting μ_m and σ_m^2 as local mean and local variance of P_{raw} respectively, v^2 as the mean of local variance σ_m^2 . P_{wiener} is the denoising result after wiener filtering.

One of the advantages of Wiener filter is that it can be adaptive to signal, provided the patch size of the filter, which suggests its clinical value. It is valuable to mention that Wiener filter exploits the correlations among neighbour pixels inside a patch, which is absolutely different from BM3D denoising algorithm.

2.3 Noise Reduction with Angle Domain

As mentioned above, strong correlations which exist among data from different detectors in detector domain, could be exploited for denoising with a Wiener filter. Data correlations in angle domain, however, are much more difficult to model. In common sense, it will achieve a better denoising performance to take use of more information of noisy data. However, in CBCT, filtering in a 3D projection volume will lead to a severe image blur in the angle direction when taking angle domain into consideration. Because of the blur in angle direction, streak artifacts may be induced in the reconstruction image.

2.4 Image Enhancement Processing

Generally speaking, structures of the reconstructed image with denoised projection data will be slightly smoothed, whereas in some cases these smoothed small structures, such as root canal and bone trabecula, play a crucial role in disease diagnosis with dental CBCT. In an attempt to to enhance the contrast/details, in this work, a simple 3D filter is designed as follows.

$$\mathbf{H}(x, y, z) = [\mathbf{f}(x, y, z) + \Delta\mathbf{f}(x, y, z)] * \mathbf{G}(x, y, z) \quad (2)$$

where $\mathbf{f}(x, y, z)$ represents the volumetric image, we denote by $\Delta\mathbf{f}(x, y, z)$ the Laplace operation of the reconstructed volume $\mathbf{f}(x, y, z)$, $\mathbf{G}(x, y, z)$ is a Gaussian filter. The operator $*$ represents a convolution operation. It is well-accepted the Laplacian operator is very sensitive to high frequency components which correspond to structures/details in images. Consequently, the first term in Eq. (2) could be regarded as an enhancement operation on images. Unavoidably, noise will also be strengthened by this filter, and hence, a Gaussian filter is utilized to suppress the emerge of noise.

Table 1. System Configuration of Dental CBCT

System configuration	Parameter
Distance from source to detector	650 mm
Distance from source to rotation center	300 mm
Detector pixel number	940 × 752
Detector pixel size	254 μm
Reconstruction dimensions	512 × 512 × 300
Scan angle	360°

2.5 Experiments

Two groups of real CBCT data, scanned with a patient and a physical phantom, respectively, were used to demonstrate the efficacy of the proposed projection denoising algorithm and image enhancement algorithm. Geometry parameters can be found in (Table 1) which is for a typical dental CBCT geometry. It is valuable to mention that a rotating mechanical error exists during scanning which would potentially lead to a distorted reconstruction. Hence, by taking this error into consideration, a new backward projection operator is fed into the standard FDK algorithm so as to deliver a high quality reconstruction.

In this work, a 5×5 patch was adopted in Wiener filter for both data. As for enhancement algorithm, the scale parameters corresponding to Laplacian operator and Gaussian operator were 0.5 and 3, respectively. For the purpose of comparison, BM3D [10] and BM4D [11] algorithm were also used to denoise the data in detector domain with a projection by projection fashion and the whole volume one time, respectively. Block size for both was 3×3 . Then all of the denoised projections were fed into a standard FDK algorithm to reconstruct the whole volume, followed by the enhancement algorithm. We will compare all of these reconstructions visually.

3 Results

The results of denoising in detector domain are presented in the following. The phantom data is showed in the top of Fig. 1 and the bottom illustrates the patient data. The left column displays the raw projection of a certain angle in Fig. 1. The denoising results in detector domain are demonstrated in the middle column. To visually demonstrate the denoising performance in detector domain the subtracted images are illustrated in (c) and (f) in a gray scale $[-0.3, 0.2]$. It can be seen that wiener filtering could remove the noise while reserve the structures as more as possible.

The obvious denoising consequence with wiener filter compared with the raw data reconstruction of slice 265 for physical phantom are illustrated in Fig. 2. To evaluate the performance of wiener filtering, different denoising

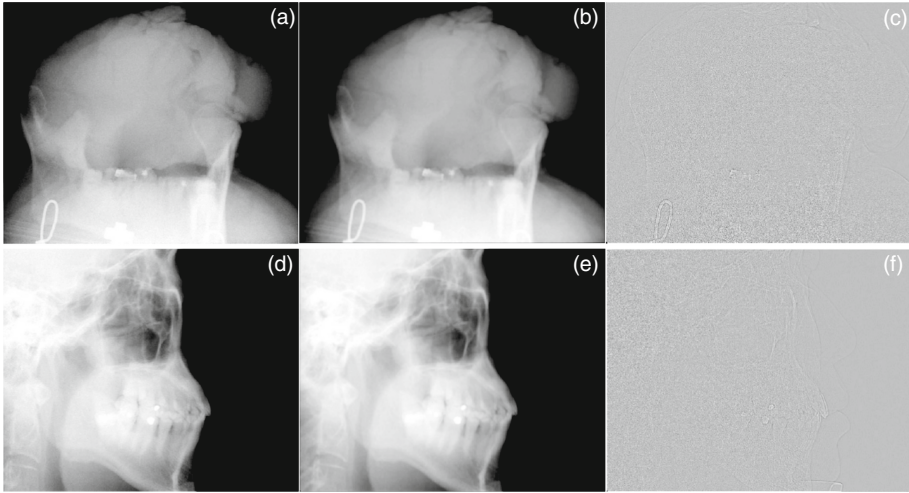


Fig. 1. Denoising results in detector domain by Wiener filter. The left column presents the raw projection in one angle. The results of denoising in detector domain are demonstrated in the middle column. The subtracted image are illustrated in (c) and (f) in the gray scale window $[-0.3, 0.2]$

approach are demonstrated for comparison. Figure 3 depicts slice 250 of volumetric reconstructions with denoised projections corresponding to Wiener-Filter/WienerFilter+Enhancement algorithm/BM3D/BM4D from left to right respectively. Figure 3 reveals that denoised projections with wiener filter could deliver a reconstruction with compromise between noise and resolution in contrast with those of BM3D and BM4D approach. Moreover, some streak artifacts still exist on the reconstructions associated with BM3D/BM4D denoising algorithm, while reconstructions corresponding to Wiener filter/Wiener filter + Enhancement appears to be much better. The sub-figs in Fig. 4 are in the same arrangements as Fig. 3. As showed in (c) of both Figs. 3 and 4, the structures are distinctly intensified by image enhancement processing. To illustrate the improvement of enhancement further, Figure 5 plot the profile across the boundary between soft tissue and bone as indicated by the red line in Fig. 4(b) and (c). It is apparent that reconstructions after processed with an enhancement filter has a better contrast, as indicated by the red arrows in Fig. 5.

4 Discussion

In this work, Wiener filter is used to denoise projection data in detector domain and leads to a reconstruction with good compromise between noise and resolution. As no block matching process is involved in Wiener filter denoising algorithm, its computation efficiency is much higher than that of block matching denoising algorithms, such as BM3D/BM4D. This provides an insight into its clinic utility where computation efficiency is of high importance.

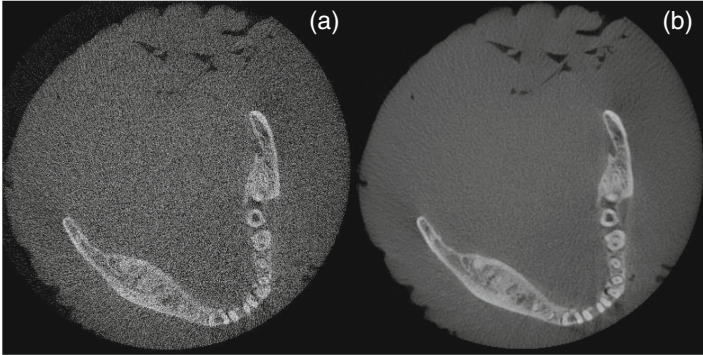


Fig. 2. Phantom reconstruction results before and after denoising via FDK algorithm in gray scale window $[0, 0.5]$. The raw data reconstruction is demonstrated in (a). (b) is reconstructed from the data after wiener filter denoising in detector domain.

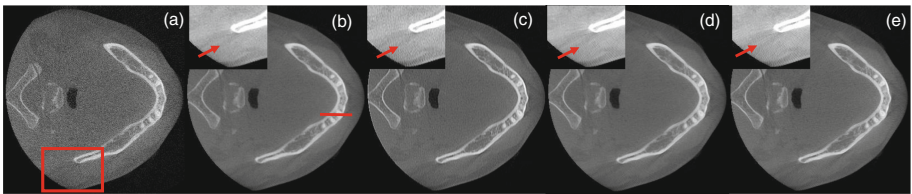


Fig. 3. Reconstructed images at slice(slice=250) of different denoising algorithm. (a) is displayed the raw data reconstruction. (b) and (c) present the reconstructed image after wiener filtering while (c) is followed by image enhancement processing. BM3D and BM4D denoising algorithm is utilized to (d) and (e) respectively. All the reconstructed image is showed at the same gray scale window $[0, 0.6]$. The insets are zoomed-in views of the red rectangle region in gray scale window $[0, 0.3]$.

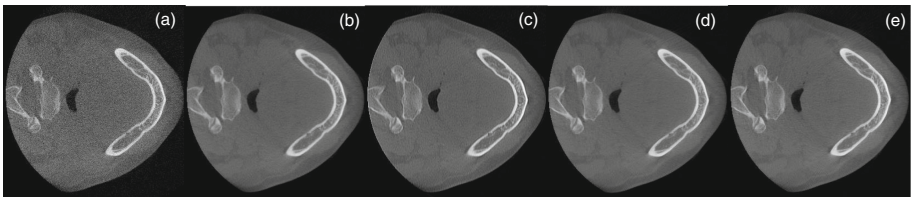


Fig. 4. Contrasted denoising results (slice=270) containing (a) with among raw data reconstructed image, (b) with reconstruction after wiener filtering, (c) with denoising reconstruction after enhancement processing, (d) and (e) with reconstruction after BM3D and BM4D denoising respectively. The different images are at the same gray scale window $[0, 0.6]$.

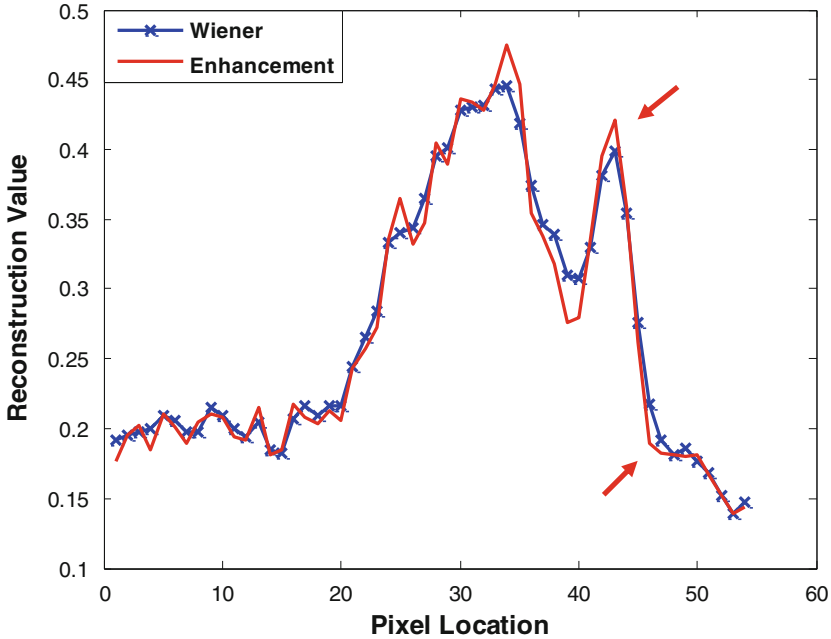


Fig. 5. Performance of image enhancement processing. The profile for the line indicated in Fig. 3(b), showing the values for image enhancement and wiener filter(*).

Moreover, unlike BM4D denoising algorithm whose performance highly depends on the input parameter, wiener filter is adaptive to signal providing the patch size, in this work, for both data, a 5×5 patch is utilized for denoising. This excellent property is crucial in clinic.

In general, the more information we take use of, the higher denoising performance is expected. However, as what we demonstrated, the combination of Wiener filter and enhancement filter could deliver a reconstruction with comparable trade-off between noise and resolution as that of BM4D which has been proved to be a very effective algorithm, which suggests that information among different views is very hard to model.

In order to reserve some fine structures in reconstructions resulted from denoised projection, in this work, an enhancement filter was designed. However, noise will also be strengthened during this process. How to design an adaptive enhancement algorithm is our future topic.

As there were only two sets of patient data examined in this study, it is apparent that the accuracy and robustness of the technique needs further assessment.

5 Conclusion

In this work, a simple but effective Wiener filter was employed to denoise data in detector domain, and then the reconstruction with denoised projection was

fed into an enhancement algorithm to strengthen small structures. Experimental results demonstrated that the proposed simple combination could achieve a comparable performance with BM4D denoising algorithm but better than that of BM3D denoising algorithm. Moreover, the proposed algorithm is very computation cost saved which is of high importance in clinics.

Acknowledgement. This work was supported in part by National Natural Science Foundation of China (NSFC) under No. 61172163, 90920003, 61302136 and 61401349, in part by Natural Science Basic Research Plan in Shaanxi Province of China (Program No. 2014JQ8317)

References

1. Wang, J., Liang, Z., Lu, H., et al.: Recent development of low-dose X-ray cone-beam computed tomography. *Curr. Med. Imaging Rev.* **6**, 72–81 (2010)
2. Hsieh, J.: Adaptive streak artifact reduction in computed tomography resulting from excessive x-ray photon noise. *Med. Phys.* **25**, 2139–2147 (1998)
3. Kachelriess, M., Watzke, O., Kalender, W.: Generalized multi-dimensional adaptive filtering for conventional and spiral single-slice, multi-slice and cone-beam CT. *Med. Phys.* **28**, 475–490 (2001)
4. Wang, J., Li, T., Lu, H., et al.: Penalized weighted least-squares approach to sinogram noise reduction and image reconstruction for low-dose X-ray computed tomography. *IEEE Trans. Med. Imaging* **25**, 1272–1283 (2006)
5. Manduca, A., Yu, L., Trzasko, J., et al.: Projection space denoising with bilateral filtering and CT noise modeling for dose reduction in CT. *Med. Phys.* **36**, 4911–4919 (2009)
6. Elbakri, I.A., Fessler, J.A.: Statistical image reconstruction for polyenergetic X-ray computed tomography. *IEEE Trans. Med. Imaging* **21**, 89–99 (2002)
7. Xu, Q., Yu, H., Mou, X., Zhang, L., Hsieh, J., Wang, G.: Low-dose X-ray CT reconstruction via dictionary learning. *IEEE Trans. Med. Imaging* **31**, 1682–1697 (2012)
8. Sidky, E.Y., Pan, X.: Image reconstruction in circular cone-beam computed tomography by constrained, total-variation minimization. *IEEE Trans. Med. Imaging* **53**, 4777 (2008)
9. Daniel, L.R., William, B.: Statistics of natural images: scaling in the woods. *Phys. Rev. Lett.* **73**, 814–817 (1994)
10. Dabov, K., Foi, A., Karkovnik, V., Egiazarian, K.: Image denoising by sparse 3-D transform-domain collaborative filtering. *IEEE Trans. Med. Imaging* **16**, 2080–2095 (2007)
11. Maggioni, M., Katkovnik, V., Egiazarian, K., Foi, A.: A nonlocal transform-domain filter for volumetric data denoising and reconstruction. *IEEE Trans. Med. Imaging* **22**, 119–133 (2013)